Chem
Europ
European C
Societies P

Check for
updates

▌ Electro, Physical & Theoretical Chemistry

Prelude to Molecular Dynamics-II: Investigation of Potential Energy Surfaces Using Gaussian Charge Models

Johnross V. Albuquerque* and Rajendra N. Shirsat[a]

The current work demonstrates the application of topography-based Gaussian charge models (GCMs) in studying potential energy surfaces of molecular dimers of water, ammonia, acetylene and benzene in addition to water-ammonia, water-acetylene, ammonia-acetylene, water-benzene, ammonia-benzene and acetylene-benzene complexes. Investigations are also carried for trimer systems of water, ammonia and their mixed compositions. The predicted geometries are in good agreement with those derived from quantum mechanical (QM) calculations and the interaction energy values forecasted deviate not more than ± 2 kcal/mol from respective QM counterparts.

1. Introduction

Hydrogen bonding and solvation are important phenomena in biological processes. In addition to holding two helical chains of nucleotides in deoxyribose nucleic acid together, the former force along with the latter also govern various types of interactions viz. ions with solvents, water with bio-molecules, protein folding etc.[1,2] In such situations, the electrostatic term is the major contributor to the total interaction energy (IE), especially at larger separation distances.[3] Though quantum mechanical (QM) methods viz. effective fragment potential are capable of handling interactions in large systems,[4] the same can be achieved by the use of point charge models (PCMs). Some examples presented hereafter demonstrate the usefulness of PCMs. The EPIC (Electrostatic Potential for Intermolecular Complexation) model has been helpful in studying hydration patterns of formaldehyde, methanol, cyclopropane, formamide and uracil molecules.[5] Interaction energies (IEs) and predicted structures of hydrated complexes were found to be in good agreement with corresponding QM counterparts. These geometries when used for QM calculations were found to converge faster. The water (H_2O) models (consisting of positive point charges placed at hydrogen sites and a negative charge along the C_2 axis) developed by Yu and Gunsteren,[6] could simulate various properties of liquid water (viz. heat capacity, self-diffusion constant, thermal expansion coefficients) at various thermodynamic states. Such predictions were found to correlate well with experimental results and theoretical values derived from QM computations. Irrespective of the methods employed to derive charges on atoms,[7–9] such PCMs are incapable of reproducing the topographical features of the Molecular Electrostatic Potential (MESP), due to lack of continuous charge component.[10]

The MESP due to a molecule at point **r**, in its vicinity is expressed in atomic units by Eq. (1) where the first term denotes the contribution of nuclei with charges {Z_i} located at {R_i}.[11] The second term arises due to electrons where $\rho(r')$ corresponds to the electron density function.

$$V(\mathbf{r}) = \sum_{i=1}^{N} \frac{Z_i}{|\mathbf{r} = \mathbf{R}_i|} - \int \frac{\rho(\mathbf{r}')}{|\mathbf{r} - \mathbf{r}'|} d\mathbf{r}' \qquad (1)$$

The rich topographical features of Eq. (1) are brought out in terms of critical points (CPs) - points where the first order partial derivatives vanish i.e. $\frac{\partial V}{\partial x_i} = 0$ for i = 1, 3. CPs are then characterized by nature of three eigenvalues {λ_i} obtained from corresponding Hessian matrix H (matrix of second order partial derivatives with elements $H_{ij} = \frac{\partial^2 V}{\partial x_i \partial x_j}$) evaluated at the CPs. If at least one of the eigenvalues is zero then, that CP is said to be degenerate. A nondegenerate CP exists when all eigenvalues are nonzero; and is represented as (R,σ) where rank (R) denotes number of non zero eigenvalues. Signature (σ) is obtained from algebraic sum of the signs of eigenvalues. Based on (R,σ) values, four types of nondegenerate CPs are possible for MESP scalar field: (3,+3), (3,−3), (3,+1) and (3,−1). The negative-valued (3,+3) CP corresponds to local minimum and signifies presence of lone pairs/π bonds.[12] Gadre and coworkers have proven the absence of non-nuclear (3,−3) type of CP.[13] Each bonded pair of atoms is indicated by (3,−1) CP.[14] A negative-valued (3,+1) CP is found to connect two nearest minima.[15]

Gadre and Shrivastava initially developed Gaussian charge models (GCMs) to reproduce topographical characteristics of ammonia (NH_3) and H_2O molecules.[16] Similar topography-based models were also developed for molecules like ethene, methanol, hydrogen sulphide and benzene (C_6H_6).[17] The earlier study from our laboratory dealt with development of topography-based GCMs and demonstrated their reliability to be employed for molecular dynamics simulations as they were capable of predicting correct geometries of water dimer $(H_2O)_2$

[a] *J. V. Albuquerque, Prof. R. N. Shirsat*
School of Chemical Sciences, Goa University, Taleigao Plateau, Taleigao
Goa. 403 206 India
E-mail: johnross.albuquerque@gmail.com

ChemistrySelect

Full Papers
doi.org/10.1002/slct.202002418

Chemistry Europe
European Chemical
Societies Publishing

and benzene-water complex ($C_6H_6...H_2O$).[18] In continuation with the same, the present study aims in rectifying the underestimated IE values reported for mentioned molecular systems and investigating potential energy surfaces (PESs) of several other interacting molecules using GCMs.

2. Computational Methotology

For benefit of readers, this section briefly describes the development of GCMs discussed in reference no. 18. Prior to GCM development, it is important to know about the various topographical features of MESP exhibited by given molecule under consideration. The corresponding molecular geometry is first optimized at the second order Møller Plesset (MP2) perturbation theory using 6–31G(d,p) basis set. The computational chemistry software Gaussian 03 is used for this purpose.[19] Optimized geometry coordinates, occupied molecular orbital coefficients and basis set information are then employed to locate and characterize MESP CPs using the software INDPROP.[20] The GCM is then constructed by placing positive point charges at nuclei sites and s-type Gaussians associated with negative charges (preferably) at coordinates corresponding to negative-valued $(3,+3)$ CPs. The model parameters: {point charges, Gaussian exponents, Gaussian locations} are optimized to obtain correct MESP topography, especially in the negative $V(\mathbf{r})$ region. For convenience, GCM parameters of H_2O, NH_3, acetylene (C_2H_2) and C_6H_6 molecules considered in this study are displayed in Table 1. Formula for computing IE using GCMs (IE_{GCM}) is described in supporting information (SI).

In the first phase, H_2O and NH_3 GCMs were used to predict minimum energy geometries of $(H_2O)_2$ and ammonia dimer $(NH_3)_2$. Use of spherical enclosures around each GCM prevents them from interpenetrating into each other. The energy minimization process occurs by keeping one model in fixed position and subjecting the other towards rotation/translation till lowest value of IE_{GCM} is obtained. A detailed description of this process is also available in reference 18. Unlike the $(H_2O)_2$ case, a higher basis set like 6–31+G(d,p) was necessary to obtain structure of $(NH_3)_2$. To maintain consistency, all QM results are reported at MP2/6-31+G(d,p) level of theory.

Frequency calculations were performed to confirm nature of corresponding optimized geometries. The QM calculations are done using Gaussian 03 suite of programs.[19] The radii of spherical enclosures $\{R_O\}$ and $\{R_N\}$ for H_2O and NH_3 GCMs are chosen such that they reproduce the binding energy (BE) and IE free from basis set superposition error (BSSE) at MP2/6-31+G(d,p) level for respective dimer geometries. Using mentioned GCM parameters and spherical enclosures, the BE and BSSE-free IE values are predicted for ammonia-water ($NH_3...H_2O$) complex. The minimum energy geometry of ($NH_3...H_2O$) predicted by GCMs is then subjected towards geometry optimization at MP2/6-31+G(d,p) level of theory. Results from the two approaches are compared. The study is then extended to acetylene dimer $(C_2H_2)_2$, benzene dimer $(C_6H_6)_2$ and other related systems.

Table 1. GCM parameters of water, ammonia, acetylene and benzene molecules. Darkened circles represent s-type Gaussian sites associated with charges {q_G} and exponent α. The ball-and-stick model is used to represent molecular framework constructed from positive point charges.

Model	Parameters

Water

C_2

q_O 4.6359
q_H 0.5795
0.0367 Å
52.9°
$\alpha = 0.3137$
$q_G = -5.7949$

Ammonia GCM-1

C_3

$\alpha = 0.3850$
$q_G = -0.2379$
1.0400 Å
q_N 0.1665
112.7°
q_H 0.0238

Ammonia GCM-2[a]

q_N 4.3598
q_H 0.3966
$\alpha = 0.2665$
$q_G = -5.5495$

Acetylene[a]

q_H 0.0502
q_C 0.9466
$\alpha = 0.1175$
$q_G = -2.0941$

Benzene[b]

$\alpha = 3.0$
$q_G = -0.00695$
q_H 0.0020
q_C 0.0119

[a] Gaussian position at centre of mass [b] refer SI for details.

ChemistrySelect

Full Papers
doi.org/10.1002/slct.202002418

Chemistry
Europe
European Chemical
Societies Publishing

3. Results and Discussion

3.1. Preliminary investigation

3.1.1. Water dimer

Using a spherical enclosure (of radius R_O originating from oxygen site) around water GCM, a linear hydrogen bonded structure is predicted for $(H_2O)_2$ as portrayed in Table 2, entry 1. One of the GCMs behaves as hydrogen (H) donor and the other as an H acceptor. This predicted orientation is in good agreement with experimentally observed structure derived from molecular beam spectroscopy,[21] and QM calculations reported by several researchers.[22] Based on optimized geometry of $(H_2O)_2$ at MP2/6-31+G(d,p) level of theory, the intermolecular oxygen-oxygen distance $\{R_{O-O}\}$ is about 2.9147 Å. For $R_O = 1.455$ Å, the GCMs predict BE of about -7.48 kcal/mol. When R_O equals 1.62 Å, the predicted IE value agrees well with its BSSE-free counterpart.

3.1.2. Ammonia dimer

Structure of $(NH_3)_2$ (Table 2, entry 2) predicted by the newly developed NH_3 GCM (Table 1, entry 3) was found to be in good agreement with those reported by various groups.[23] The shortcomings of ammonia GCM-1 (from Table 1) are described in SI. As in the case of H_2O GCM, the ammonia GCM was employed using a spherical enclosure. The intermolecular nitrogen-nitrogen distance $\{R_{N-N}\}$ in optimized geometry of $(NH_3)_2$ is about 3.2422 Å. Considering $R_N = 1.62$ Å, the GCMS predict BE of -4.61 kcal/mol and if R_N equals 1.845 Å, then, the predicted BSSE-free energy is about -2.80 kcal/mol. With suitable R_O and R_N values chosen for H_2O and NH_3 models, the interaction between these two molecules is investigated hereafter.

3.1.3. Ammonia-water complex

Minimum energy structure of $NH_3\ldots H_2O$ complex predicted by GCMs is portrayed in Table 2, entry 3 wherein the two hydrogen atoms labeled by asterisk symbols are in 'cis' orientation. At MP2/6-31+G(d,p) level of theory, the 'trans' orientation is found to be slightly more stable than the 'cis' orientation. QM calculations reported in the work of Sälli and co-workersalsoconfirm this observation.[24] The predicted energies are in good agreement with QM counterparts.

3.1.4. Acetylene dimer, acetylene-water and acetylene-ammonia complexes

A single s-type Gaussian charge distribution placed at the centre of mass in C_2H_2 GCM restores the topographical features of MESP viz. ring of degenerate CPs and $(3,-1)$ CPs between C−H and C≡C bonds (refer SI for insights on GCM development). The model was then employed to find minimum energy structure of $(C_2H_2)_2$ with van der Waal (vdW) type of enclosure constructed from spheres (of radius R_C) originating from carbon atoms. The GCMs predict a T-shape geometry (Table 2, entry 4)

which is confirmed from earlier,[25] and present QM calculations. The IEs obtained for choice of $R_C = 1.7$ and 1.9 Å are also displayed in Table 2.

Owing to the acidic nature of hydrogen atoms in acetylene, this molecule is expected to behave as a H donor during its interaction with either H_2O or NH_3 molecules. The GCMs successfully predict such behavior (Table 2, entries 5 and 6) which agree well with current QM calculations and those reported by researchers.[26] More importantly, the choice of R_C and R_O values determine the angle $\{\mathring{\alpha}\}$ between C_2 axis of H_2O and C_∞ axis of C_2H_2 in acetylene…water complex. In predicting the BE of the complex, value of angle $\mathring{\alpha}$ agrees well with that obtained from corresponding QM counterpart. However $\mathring{\alpha}$ is close to zero when predicting BSSE-free IE.

The various R_C, R_N and R_O values proposed for C_2H_2, NH_3 and H_2O models work well in predicting BE and BSSE corrected IE values (which deviate not more than ± 2 kcal/mol from respective QM counterparts).

3.1.5. Benzene dimer

Extensive work on aromatic-aromatic interactions ($(C_6H_6)_2$ being the simplest example) has been carried out by Burley and Petsko, who defined these interactions as those between phenyl rings whose centroids are separated by a distance of 4.5–7.0 Å with energy of formation in the range of -0.6 to -1.3 kcal/mol.[27] Such a separate class of interactions contributes to some extent towards stability of protein structures (more dominant when protein contains large number of aromatic fragments). These interactions are divided into two categories: π-π stacking resulting from face-to-face orientation of aromatic rings and the C-H interactions due to edge-to-face orientation of aromatic substrates. Based on the electrostatic model proposed by Hunter and Sanders, the π-π stacking in $(C_6H_6)_2$ is due to repulsion between π electrons and attraction between positively charged benzene rings with π electrons.[28] The coulombic interactions between aromatic hydrogen atoms and π electrons of different rings result to C−H interactions. Tsuzuki and co-workers pointed out that the electrostatic interactions favor the T-shape structure of $(C_6H_6)_2$ while dispersion energy (a ubiquitous weak attractive force) directs the benzene rings in face-to-face geometry.[29]

Though inappropriate to enclose the entire benzene GCM by a single sphere of radius R_{mol} originating from centre of mass and employ the same to study PES of $(C_6H_6)_2$, such implementation has yielded some important observations which are displayed in Figure 1.

1) With $R_{mol} = 2.6450$ Å, energy minimization starting from the face-to-face orientation of $(C_6H_6)_2$ results to the T-shape geometry with C_{2v} point group.
2) With a different R_{mol} value ($R'_{mol} = 2.4772$ Å) however, a T-shape geometry with C_2 point group is obtained.
3) The above results are observed even when a vdW type of enclosure (surface generated from spheres of radii $\{R_C\}$ originating from carbon atoms) is employed around benzene GCM, provided value of R_C is greater than 1.8 Å.

ChemistrySelect

Full Papers
doi.org/10.1002/slct.202002418

Chemistry
Europe
European Chemical
Societies Publishing

Table 2. Summary of preliminary investigation carried out using GCMs. The dots represent *s*-type Gaussians in respective models.

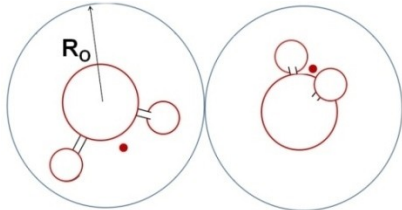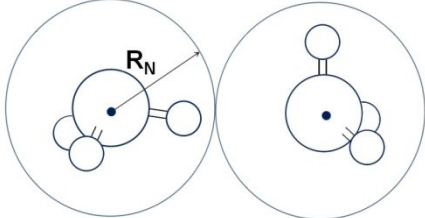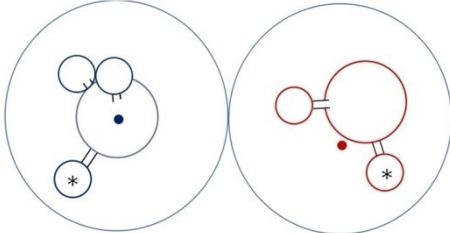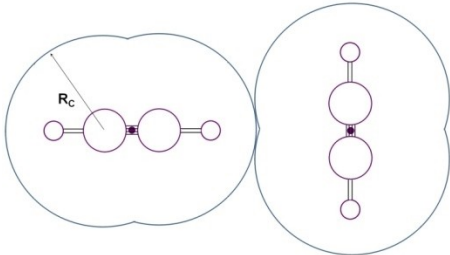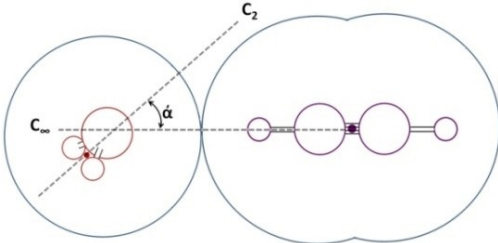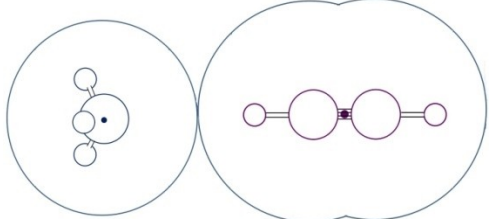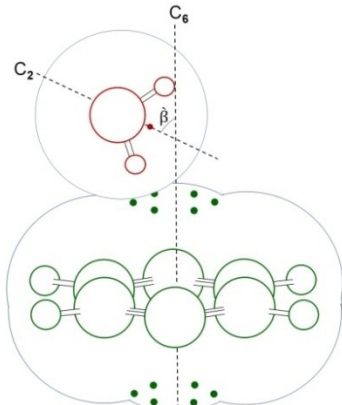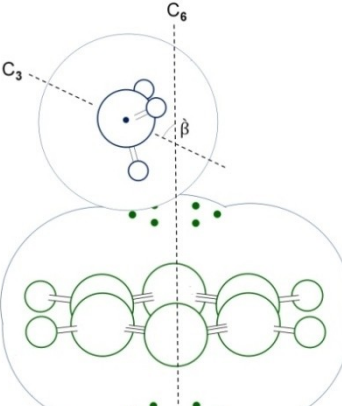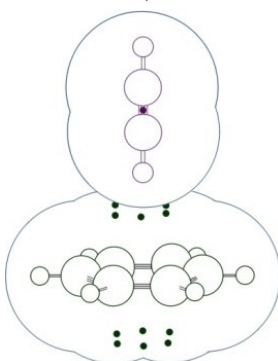| Sr. No.	Molecular system	Geometry from energy minimization calculations using GCMs	Interaction Energy (kcal/mol)
1	Water dimer		-6.38 MP2/6-31$+$G(d,p) -4.78 including BSSE correction -7.50 GCMs; $R_O = 1.455$ Å -4.75 GCMs; $R_O = 1.64$ Å
2	Ammonia dimer		-4.00 MP2/6-31$+$G(d,p) -2.75 including BSSE correction -4.61 GCMs, $R_N = 1.62$ Å -2.80 GCMs; $R_N = 1.845$ Å
3	Ammonia-water complex		-8.20 GCMs; $R_O = 1.455$ Å and $R_N = 1.62$ Å -5.08 GCMs; R_O and R_N values of 1.64 and 1.845 Å -7.83 (cis) MP2/6-31$+$G(d,p) -6.07 (cis) including BSSE effect -7.85 (trans) MP2/6-31$+$G(d,p) -6.07 (trans) including BSSE effect
4	Acetylene dimer		-1.95 GCMs; $R_C = 1.7$ Å -1.20 GCMs; $R_C = 1.9$ Å -1.98 MP2/6-31$+$G(d,p) -0.91 including BSSE correction
5	Acetylene-water complex		-3.50 GCMs; $R_C = 1.7$ Å and $R_O = 1.455$ Å; $\dot{\alpha} = 20.92°$ -2.15 GCMs; $R_C = 1.9$ Å and $R_O = 1.64$ Å; $\dot{\alpha} = 0.13°$ -4.09 MP2/6-31$+$G(d,p); $\dot{\alpha} = 17.21°$ -2.56 including BSSE correction
6	Acetylene-ammonia complex		-3.76 GCMs; $R_C = 1.7$ Å and $R_N = 1.62$ Å -2.39 GCMs; $R_C = 1.9$ Å and $R_N = 1.845$ Å -4.81 MP2/6-31$+$G(d,p) -3.10 including BSSE correction

ChemistrySelect

Full Papers
doi.org/10.1002/slct.202002418

Chemistry
Europe
European Chemical
Societies Publishing

Table 2. continued

Sr. No.	Molecular system	Geometry from energy minimization calculations using GCMs	Interaction Energy (kcal/mol)
7	Benzene-water complex		-2.81 GCMs; $R_C = 1.9$ Å and $R_O = 1.455$ Å, $\beta = 66.98°$ [a]R (ring centre, O) $= 3.3550$ Å -4.08 MP2/6-31+G(d,p) $\beta = 42.11°$ R (ring centre, O) $= 3.3738$ Å -2.16 including BSSE correction
8	Benzene-ammonia complex		-1.54 GCMs; $R_C = 1.9$ Å and $R_N = 1.62$ Å; $\beta = 78.17°$ R (ring centre, N) $= 3.7450$ Å -3.07 MP2/6-31+G(d,p); $\beta = 42.11°$; R (ring centre, N) $= 3.3738$ Å -1.23 including BSSE correction
9	Benzene-acetylene complex		-1.16 GCMs; with $R_C = 1.9$ Å for C_6H_6 and $R_C = 1.7$ Å for C_2H_2 model -0.89 using GCMs; $R_C = 1.9$ Å for both models -4.26 MP2/6-31+G(d,p) -1.67 including BSSE correction

[a] R(ring centre, X): distance between ring centre and X type of atom where X $=$ O, N.

4) For R_C values less than 1.8 Å, interaction between hydrogen end of one GCM and Gaussian center of the other is observed. For example, when R_C equals 1.5 Å, energy minimization of benzene GCMs results in a structure having C_s point group.

It is more appropriate to consider the vdW type of enclosure around C_6H_6 GCM which envelopes all s-type Gaussians. In this context, the surface generated from spheres at carbon sites of radius $R_C = 1.9$ Å appears to be a good choice.

The face-to-face and T-shaped geometries are stationary points along the PES of $(C_6H_6)_2$ at MP2/6-31+G(d,p) level of theory. The IE_{GCM} values predicted for mentioned stationary points are found to be overestimated (as shown in Table 3). It is hoped that the C_6H_6 GCM predicts reasonable IE values on interacting with H_2O, NH_3 and C_2H_2 molecules.

ChemistrySelect

Full Papers
doi.org/10.1002/slct.202002418

Chemistry Europe
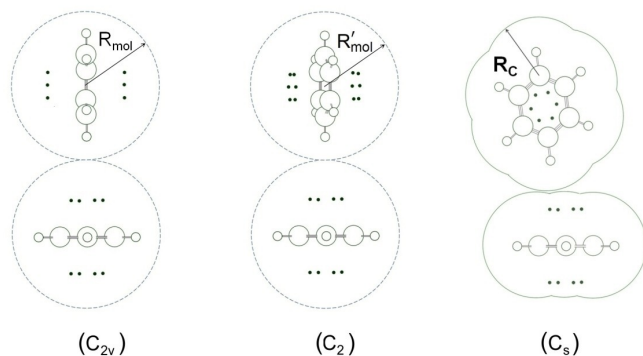European Chemical
Societies Publishing

Figure 1. Effect of employing different enclosures around benzene GCM on predicted minimum energy structure of benzene dimer. The first two structures on the left are obtained by using spherical enclosures of radii 2.6450 and 2.4772 Å respectively. The right hand side structure is the result of using vdW surface around benzene GCM. Point group of respective geometries are displayed in parenthesis. Refer text for more details.

Table 3. Interaction energies of some stationary points along PES of benzene dimer obtained via. QM calculations at MP2/6-31+G(d,p) level of theory and GCMs.

Geometry	Distance between ring centroids (Å)	BE (kcal/mol)	IE (BSSE free) (kcal/mol)	IE using GCMs (kcal/mol)
Face-to-face	3.8457	−4.00	−1.32	0.56
T-shape (C_{2v})	4.8375	−4.88	−1.71	−0.03
T-shape (C_2)	4.8199	−4.88	−1.65	−0.04

3.2. Interaction of benzene with water, ammonia and acetylene molecules

In both: $C_6H_6…H_2O$ and benzene-ammonia ($C_6H_6…NH_3$) complexes, one of the hydrogen atoms belonging to H_2O and NH_3 molecules is found to interact with the π cloud of aromatic substrate (Table 2, entries 7 and 8). Based on the predicted IE_{GCM} values, one can conclude that the H_2O molecule is strongly bound to C_6H_6 as compared to NH_3. Earlier reports and current QM calculations support this inference.[30] The minimum energy structure of $C_6H_6…H_2O$ complex was obtained at MP2/6-31+G(d,p) level of theory.

The underestimated IE_s,[18] reported for several stationary points along PES of $C_6H_6…H_2O$ complex at MP2/6-31G(d,p) level of theory (Table 4, column 2) have been rectified (Table 4, column 4) by using vdW/spherical enclosures for respective GCMs. These stationary points were also optimized at MP2/6-31+G(d,p) level of theory and corresponding geometries are displayed in column 5 of Table 4. The orientation of H_2O with respect to C_6H_6 remains identical in almost all geometries except in the first row of Table 4. The right hand side structure resembles the minimum energy geometry of $C_6H_6…H_2O$ complex reported in Table 2 (with respect to orientation of

hydrogen atoms of water). GCMs also predict lowest BE/BSSE-free IE for this geometry.

The structure of benzene…acetylene complex predicted by GCMs is displayed in Table 2, entry 9 wherein C_2H_2 acts as a H donor and C_6H_6 as H acceptor. The BE prediction for this complex is done using vdW enclosures whose R_C value equals 1.7 Å for C_2H_2 and 1.9 Å for C_6H_6. For BSSE-free IE prediction, value of R_C equals 1.9 Å in both models. It is seen that the GCM prediction in either case is overestimated.

3.3. Interactions between different compositions of water and ammonia molecules

Water and ammonia GCMs successfully predicted geometries of respective trimers along with structures of $(NH_3)(H_2O)_2$ and $(NH_3)_2(H_2O)$ complexes which are presented in Table 5. It is observed that there is a good agreement between GCM predictions and QM calculations with respect to geometries of interacting systems wherein each molecule acts as H donor and H acceptor. A direct relation between number of water molecules in given system and strength of interaction is also observed (i.e. drop in the IE as the number of water molecules decrease). The GCM-predicted BEs don't vary more than ±1 kcal/mol from respective QM counterparts however the predicted BSSE-free energies show more deviations from QM values.
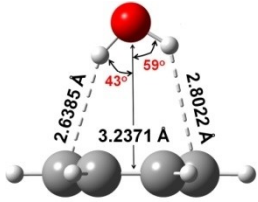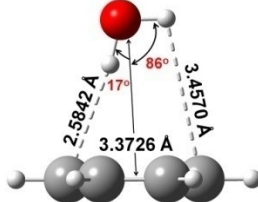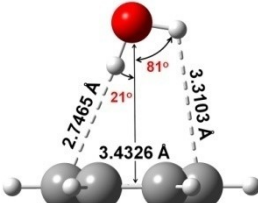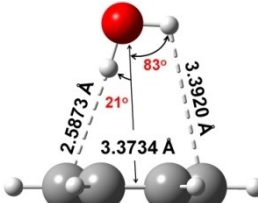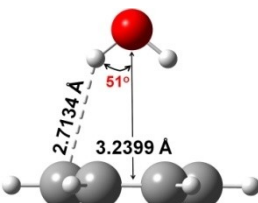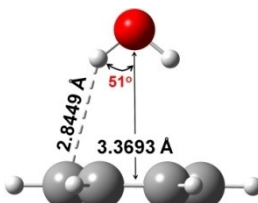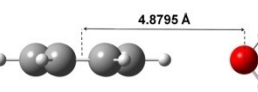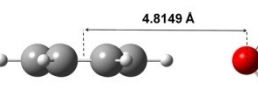
3.4. Revisiting the potential energy surfaces of water/ammonia dimers

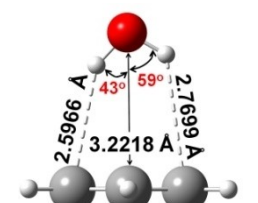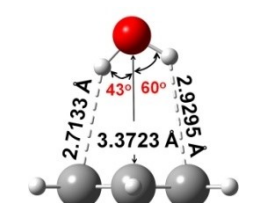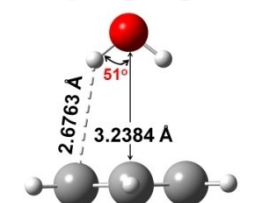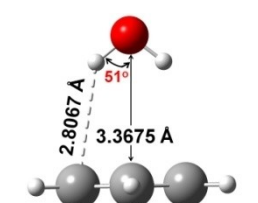The two H_2O molecules in minimum energy structure of $(H_2O)_2$ are expected to repel each other for R_{O-O} values less than 2.9147 Å and attract each other at larger separation distances. This behavior is observed when BE computed at MP2/6-31+G(d,p) level of theory is plotted as a function of R_{O-O} (Figure 2A, continuous curve). The GCMs on the other hand are incapable of mimicking this trend (Figure 2A, discontinuous curve) due to their simplistic nature (constituting of only positive point charges and Gaussians associated with negative charges). Hence it was necessary to employ appropriate enclosures while using these models to study PESs of various systems. The most widely used model to replicate short term repulsion effects in molecular simulations is the so-called Lennard-Jones (LJ) 12–6 potential term {E_{LJ}} defined by Eq. (2).[31]

$$E_{LJ} = \sum_{i<j} \varepsilon_{ij} \left[\left(\frac{\sigma_{ij}}{R_{ij}} \right)^{12} - \left(\frac{\sigma_{ij}}{R_{ij}} \right)^{6} \right] \qquad (2)$$

The first and second terms in Eq. (2) account the short-range repulsion and attraction contributions while the sum is extended to all atom pairs (i, j) of two molecules (A, B), R_{ij} being the distance between different atom pairs of molecules A and B; σ_{ij} and ε_{ij} (known as LJ parameters bearing dimensions of distance and energy) being some empirical parameters such that $\sigma_{ij} = (\sigma_i + \sigma_j)/2$ and $\varepsilon_{ij} = (\varepsilon_i \times \varepsilon_j)^{0.5}$. Including the LJ term i.e. Eq. (2) when computing IEs via. GCMs could perhaps restore the short-range repulsion effects.

ChemistrySelect

Full Papers
doi.org/10.1002/slct.202002418

**Chemistry
Europe**
European Chemical
Societies Publishing

Table 4. IEs in kcal/mol predicted by GCMs for some stationary points along PES of benzene-water complex.

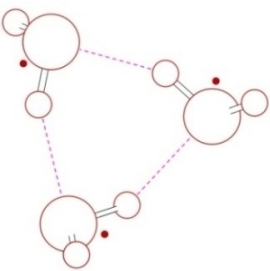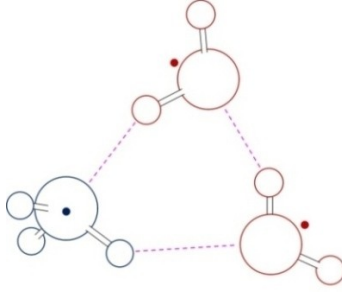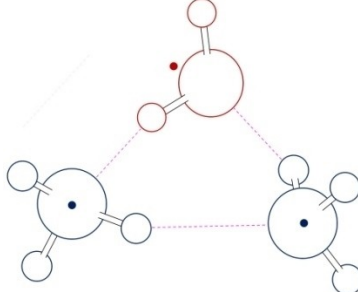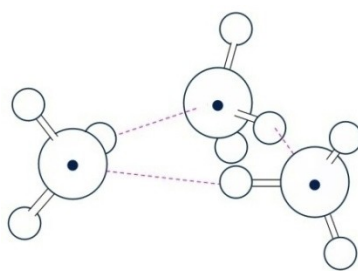| Point group	MP/6-31G(d,p) Optimized geometry	IE (kcal/mol) BE/ BSSE-free	GCMs	MP/6-31+G(d,p) Optimized geometry starting from column 2 structure	IE (kcal/mol) BE/ BSSE-free	GCMs
C_s		−4.17 −1.86	−1.45 −1.22		−4.07 −2.16	−2.26 −1.86
C_1		−3.06 −1.34	−2.21 −1.80		−4.07 −2.18	−2.20 −1.76
C_{2v}		−4.17 −1.88	−1.35 −1.14		−3.88 −2.18	−1.35 −1.14
C_{2v}		−2.13 −1.16	−0.06 −0.05		−2.56 −1.14	−0.06 −0.05
C_s		−4.17 −1.87	−1.45 −1.21		−3.91 −2.19	−1.45 −1.21
C_{2v}		−4.17 −1.88	−1.35 −1.14		−3.88 −2.18	−1.35 −1.14

In the simple case of $(H_2O)_2$, the positive valued LJ parameters $\{\varepsilon_{ij}, \sigma_{ij}\}$ from Eq. (2) are equivalent to $\{\varepsilon_{water}, \sigma_{water}\}$ as $\varepsilon_i = \varepsilon_j$, $\sigma_i = \sigma_j$ and for convenience, $\{\varepsilon_i, \sigma_i\}$ are referred to $\{\varepsilon_{water}, \sigma_{water}\}$. As spherical enclosures originating from oxygen atoms have been used for water GCMs, the same approach is continued in present context. so that the R_{ij} term in Eq. (2) corresponds to R_{O-O}. LJ parameters $\{\varepsilon_{water}, \sigma_{water}\}$ are then obtained by minimizing the objective function △defined by Eq. (3) using subroutine STEPIT.[32]

$$\Delta = \sum_{i=1}^{N} \left| \begin{array}{c} BE_i^{WF}(R_{O-O}) - \\ \left(BE_i^{GCM}(R_{O-O}) + \varepsilon_{water} \right. \\ \left. \left[\left(\frac{\sigma_{water}}{R_{O-O}} \right)^{12} - \left(\frac{\sigma_{water}}{R_{O-O}} \right)^{6} \right] \right) \end{array} \right| \quad (3)$$

The first term in Eq. (3) is the BE value of $(H_2O)_2$ obtained using QM calculation while the entire second term in brackets corresponds to its GCM counterpart, inclusive of LJ component. With respect to minimizing Eq. (3), the GCMs have to (ideally) reproduce R_{O-O} value of 2.9147 Å in $(H_2O)_2$. Also the BE values

ChemistrySelect

Full Papers
doi.org/10.1002/slct.202002418

Chemistry
Europe
European Chemical
Societies Publishing

Table 5. Minimum energy structures and IEs of three interacting molecules predicted by GCMs.		
Molecular system	Minimum energy geometry predicted by GCMs	Interaction energy (kcal/mol)
Three water molecules		−19.54 GCMs; R_O = 1.455 Å −12.25 GCMs; R_O = 1.64 Å −18.65 at MP2/6-31+G(d,p) −14.79 including BSSE correction *−17.55 BE related LJ parameters* *−13.47 BSSE-free related LJ parameters*
Two water molecules and one ammonia molecule		−18.96 GCMs; R_O = 1.455 & R_N = 1.62 Å −11.65 GCMs; R_O = 1.64 & R_N = 1.845 Å −18.59 at MP2/6-31+G(d,p) −14.59 including BSSE correction *−16.91 BE related LJ parameters* *−12.99 BSSE-free related LJ parameters*
One water molecule and two ammonia molecules		−16.20 GCMs; R_O = 1.455 & R_N = 1.62 Å −9.85 GCMs; R_O = 1.64 & R_N = 1.845 Å −16.48 at MP2/6-31+G(d,p) −12.71 including BSSE correction *−14.99 BE related LJ parameters* *−11.22 BSSE-free related LJ parameters*
Three ammonia molecules		−13.38 GCMs; R_N = 1.62 Å −8.02 GCMs; R_N = 1.845 Å −12.81 at MP2/6-31+G(d,p) −9.45 including BSSE correction *−12.93 BE related LJ parameters* *−9.53 BSSE-free related LJ parameters*

for $R_{O\text{-}O}$ values less than 2.9147 Å are expected to become less negative.

When {ε_{water}, σ_{water}} equals {3.5675 kcal/mol, 3.0307 Å}, lowest value of Eq. (3) is about 0.1735 kcal/mol. The GCM-predicted $R_{O\text{-}O}$ value in $(H_2O)_2$ turns out to be 3.0016 Å with BE of −6.41 kcal/mol. These findings are the result of constructing the objective function △using last six data entries from Table 6 and then subjecting Eq. (3) towards minimization. As seen from the energy profile diagram in Figure 2B, BE becomes less negative for $R_{O\text{-}O}$ values less than 3 Å. Similar profiles obtained for additional stationary structures of $(H_2O)_2$ having C_{2v} point group also confirm such behavior (refer Figures 3A and 3B).

Though H_2O GCMs (on incorporation with 12–6 LJ potential term) are able to mimic short-range repulsion effects, the deviation between GCM-predicted BEs and corresponding QM

values is found to increase as $R_{O\text{-}O}$ decreases. This probably is the result of considering the entire H_2O as a single hard sphere whose radius equals σ_{water}. The BE trend could change if one considers spheres for hydrogen atoms as well. Though additional studies may be required for the same, the current implementation is found to exhibit satisfactory results (discussed in upcoming sections).

LJ parameters {ε_{water}, σ_{water}} = {0.4164 kcal/mol, 3.5001 Å} replicate the BSSE-free interaction energy trend (Figure 4, Table 7) in minimum energy structure of $(H_2O)_2$. Considering these values, the GCMs predict $R_{O\text{-}O}$ value of 2.9943 Å and BSSE-free IE of about −5.06 kcal/mol.

For NH_3 GCM, LJ parameters: {$\varepsilon_{ammonia}$, $\sigma_{ammonia}$} = {2.2869 kcal/mol, 3.2860 Å} replicate the BE trend in minimum energy structure of $(NH_3)_2$. The $R_{N–N}$ distance is about 3.2287 Å

ChemistrySelect

Full Papers
doi.org/10.1002/slct.202002418
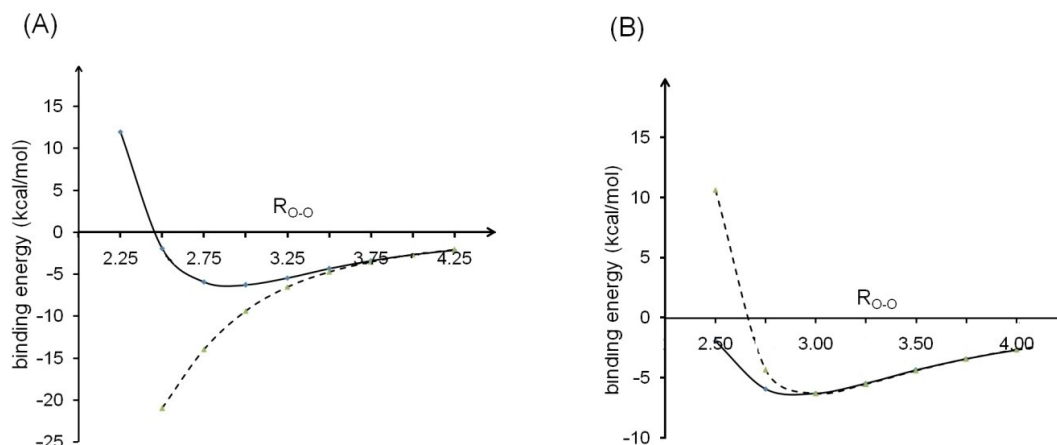
**Chemistry
Europe**
European Chemical
Societies Publishing

Figure 2. Comparison between binding energy plots for $(H_2O)_2$ obtained using GCMs (A) in absence and (B) in presence of 12–6 LJ potential term with QM calculation done at MP2/6-31+G(d,p) level of theory. The continuous and discontinuous curves depict QM and GCM behavior respectively. Data used for these plots is from Table 6.

Table 6. Binding energy as a function of intermolecular oxygen-oxygen in minimum energy structure of $(H_2O)_2$.

Value of i	R_{O-O} (Å)	[a]BE_i^{WF} (kcal/mol)	[b]BE_i^{GCM} (kcal/mol)	[c]E_{LJ} (kcal/mol)	[d]BE using GCMs (kcal/mol)
1	2.25	11.92	−20.97	105.95	84.98
2	2.50	−1.95	−13.98	24.62	10.64
3	2.75	−5.92	−9.37	5.06	−4.31
4	3.00	−6.29	−6.53	0.24	−6.29
5	3.25	−5.45	−4.72	−0.80	−5.52
6	3.50	−4.37	−3.52	−0.87	−4.39
7	3.75	−3.41	−2.69	−0.72	−3.41
8	4.00	−2.68	−2.10	−0.55	−2.65
9	4.25	−2.12	−1.67	−0.41	−2.08

[a] value obtained at MP2/6-31+G(d,p) level of theory; [b] calculated via. Eq. (S10) in SI, section S1; [c] calculated using Eq.(2) where {ε_{water}, σ_{water}} values are mentioned in main text and [d] obtained by adding column 4 values to column 5.

with BE of −4.40 kcal/mol. These values are in good agreement with corresponding QM counterparts ($R_{N–N} = 3.2422$ Å, BE = −4.0 kcal/mol) obtained at MP2/6-31+G(d,p) level of theory. The second set of parameters: {$\varepsilon_{ammonia}$, $\sigma_{ammonia}$} = {0.5983 kcal/mol, 3.6786 Å} are used for predicting IE free from BSSE. The R_{N-N} value is about 3.3489 Å with IE of −3.25 kcal/mol. The LJ parameters proposed for H_2O and NH_3 models are used to study systems involving these species. The overall summary is as follows.

1) Using LJ parameters (ε_{water}, σ_{water}) = {3.5675 kcal/mol, 3.0307 Å} and {$\varepsilon_{ammonia}$, $\sigma_{ammonia}$} = {2.2869 kcal/mol, 3.2860 Å}, the BE for $NH_3 \ldots H_2O$ complex turns out to be −7.65 kcal/mol with R_{N-O} distance of 3.0336 Å.

2) The predicted BSSE-free IE value is about −6.27 kcal/mol with intermolecular nitrogen-oxygen distance of about 3.0627 Å when following LJ parameters are used: {ε_{water}, σ_{water}} = {0.4164 kcal/mol, 3.5001 Å} and {$\varepsilon_{ammonia}$, $\sigma_{ammonia}$} = {0.5983 kcal/mol, 3.6786 Å}.

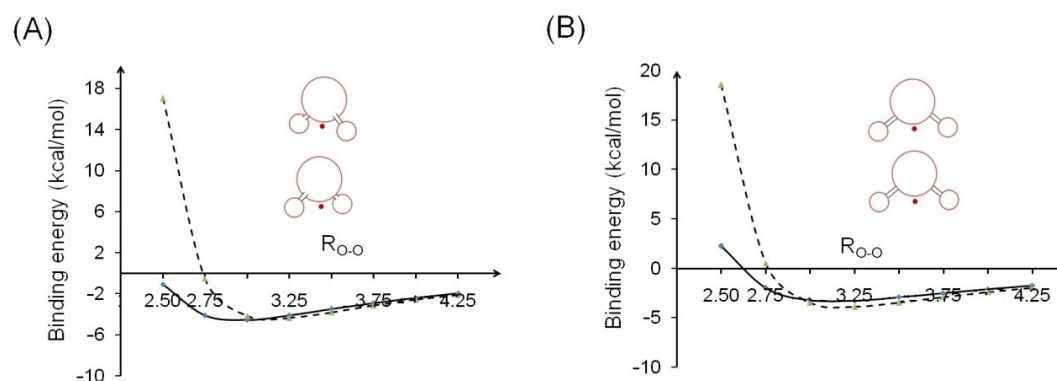**Figure 3.** Binding energy as a function of R_{O-O} in stationary structures along PES of $(H_2O)_2$ where (A) the two molecular planes are perpendicular to each other and (B) both molecules lie in the same plane. Values lying on the continuous curves are derived from QM calculations at MP2/6-31+G(g,p) level of theory while those on discontinuous are computed using GCMs (incorporated with 12–6 LJ term).
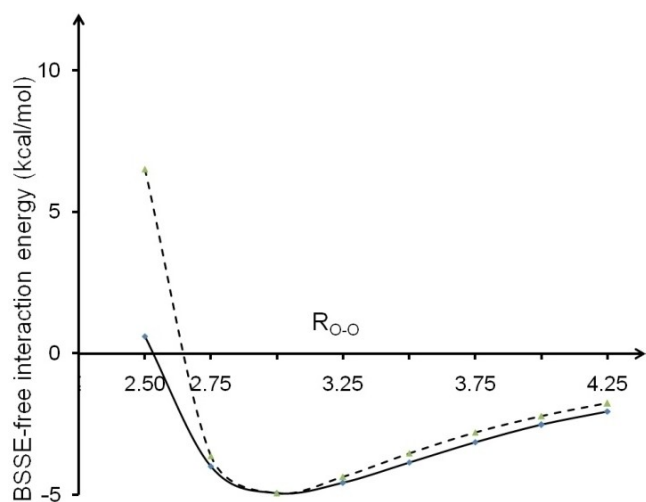
ChemistrySelect

Full Papers
doi.org/10.1002/slct.202002418

Chemistry Europe
European Chemical
Societies Publishing

Figure 4. BSSE-free interaction energy as a function of R_{O-O} in minimum energy structure of $(H_2O)_2$. The continuous curve depicts QM trend in IE computed at MP2/6-31+G(d,p) level of theory while the discontinuous curve is derived using GCMs incorporated with LJ component. Data used for this plot is available in Table 7.

Table 7. BSSE-free interaction energy as a function of R_{O-O} in $(H_2O)_2$ at MP2/6-31+G(d,p) level of theory and using GCMs with LJ parameters: {ε_{water}, σ_{water}} = {0.4164 kcal/mol, 3.5001 Å}.

R_{O-O} (Å)	BSSE-free IE at MP2/6-31+G(d,p) (kcal/mol)	BSSE-free IE using GCMs (kcal/mol)
2.50	0.60	6.50
2.75	−3.99	−3.62
3.00	−4.93	−4.93
3.25	−4.56	−4.36
3.50	−3.84	−3.52
3.75	−3.13	−2.78
4.00	−2.52	−2.20
4.25	−2.05	−1.76

3) In both cases the predicted geometry is similar to that displayed in Table 2, entry 3 (asterisk marked hydrogen atoms are in 'cis' orientation).

4) With respect to $(H_2O)_3$, $(NH_3)_3$ and those trimer systems containing different composition of H_2O and NH_3, the predicted BE/BSSE-free energies (displayed in Table 5, in 'italics' font) do not deviate more than ±1 kcal/mol. The

geometries of these systems are similar to those predicted by GCMs in the absence of LJ component.

It is interesting to note that the H_2O and NH_3 GCMs (with or without incorporating 12–6 LJ potential term) are successful in predicting geometries for $(H_2O)_3$, $(NH_3)_3$, $(H_2O)(NH_3)_2$, $(H_2O)_2(NH_3)$ type of systems and forecasts a slightly different orientation for H_2O in $NH_3…H_2O$ complex. The QM result remained unaltered on employing a triple zeta basis set like 6–311++G(d,p) but was in agreement with GCM prediction when aug-cc-pVDZ basis set was used. All mentioned systems in this section were also optimized at MP2/aug-cc-pVDZ level of theory and the IEs obtained are summarized in Table 8. Almost in all cases, the GCM predicted IEs (obtained using LJ potential term) don't vary by ±1 kcal/mol.

K. Morokuma from his theoretical investigation described five factors which play a key role in understanding origin of noncovalent interactions: electrostatics, polarization, exchange repulsion, charge transfer and coupling.[3a] Thus the total interaction energy is written as a sum of all these contributions. A detailed description on each of these terms is available in the cited reference. Based on these five components, it was possible for Morokuma to study several donor-acceptor type of complexes (viz. $(H_2O)_2$, water-hydrogen fluoride etc.) and concluded that the electrostatic component plays a vital role in complexes possessing linear X–H-Y hydrogen bonds (where X, Y are electronegative atoms like nitrogen, oxygen and fluorine). As GCMs are constructed using positive point charges and s-type Gaussian distributions associated with negative charges, they cannot be expected to account for factors other than electrostatics.

4. Conclusions

From the study presented, the GCMs are able to predict geometries of interacting molecules wherein the electrostatic component is the major contributor to the total interaction energy. The PESs of water and ammonia dimers were successfully investigated by employing spherical enclosures around respective models. Use of appropriate radii made it possible to predict BE and BSSE-free interaction energies of mentioned and several other related systems. The newly developed ammonia GCM with its s-type Gaussian centre located at nitrogen site has proven itself to be reliable by not only predicting geometry of $(NH_3)_2$ but also of various trimer systems: $(NH_3)_n(H_2O)_{3-n}$ where n takes values from 1 to 3. For acetylene and benzene GCMs, a vdW type of surface was

Table 8. BSSE-free energies for systems involving water and ammonia molecules.

Method		System						
		$(H_2O)_2$	$(NH_3)_2$	$NH_3…H_2O$	$(H_2O)_3$	$(H_2O)_2(NH_3)$	$(H_2O)(NH_3)_2$	$(NH_3)_3$
BE	GCMs without LJ	−7.50	−4.61	−8.20	−19.54	−18.96	−16.20	−13.38
	GCMs with LJ	−6.41	−4.40	−7.65	−17.55	−16.91	−14.99	−12.93
	MP2/aug-cc-pVDZ	−5.26	−3.62	−6.95	−16.36	−16.56	−14.89	−11.92
BSSE-free IE	GCMs without LJ	−4.75	−2.80	−5.08	−12.25	−11.65	−9.85	−8.02
	GCMs with LJ	−5.06	−3.25	−6.27	−13.47	−12.99	−11.22	−9.53
	MP2/aug-cc-pVDZ	−4.43	−2.73	−5.81	−13.90	−13.91	−12.21	−9.23

ChemistrySelect

Full Papers
doi.org/10.1002/slct.202002418

Chemistry Europe
European Chemical
Societies Publishing

employed - constructed using spheres occupying carbon atomic sites. There is a need to improve the benzene GCM (a task which is currently undertaken in our laboratory) with respect to predicting reasonable IE values for stationary points along PES of $(C_6H_6)_2$ though the model was found to perform quite well in predicting the strength of interaction between $C_6H_6{\ldots}H_2O$ and $C_6H_6{\ldots}NH_3$ complexes.

A major drawback of GCMs: unable to mimic repulsion effects at shorter distances is rectified by introducing a 12–6 LJ potential term when computing IEs. This is demonstrated from the studies undertaken in $(H_2O)_2$, $(NH_3)_2$ and $NH_3{\ldots}H_2O$ complexes. Irrespective of whether the LJ component is incorporated or not for computing IE_{GCM} values, the predicted geometries of complexes in either case agree with each other.

Electrostatics is found to play a major role in almost all molecular systems investigated using GCMs. It would be interesting to venture into systems wherein there is least contribution of the electrostatic component to total IE. Further studies are therefore essential to comment on the reliability of topography-based Gaussian models in such circumstances.

Supporting Information

The formula used to calculate interaction energy using topography-based Gaussian charge model is described in the supporting information. Also, geometric parameters of models discussed in the study, shortcomings of earlier published ammonia model (in reference no. 18) and data used to obtain $\{\varepsilon_{ammonia}, \sigma_{ammonia}\}$ are provided.

Conflict of Interest

The authors declare no conflict of interest.

[1] J. Watson, F. Crick, *Nature* **1953**, *171*, 737–738.
[2] P. Ren, J. Chun, D. Thomas, M. Schneiders, M. Marucho, J. Zhang, N. Baker, *Q. Rev. Biophys.* **2012**, *45*, 427–491.
[3] a) K. Morokuma, *Acc. Chem. Res.* **1977**, *10*, 294–300;b) H. Umeyama, K. Morokuma, *J. Am. Chem. Soc.* **1977**, *99*, 1316–1332;c) W. Sokalski, M. Shibata, R. Ornstein, R. Rein, *J. Comput. Chem.* **1992**, *13*, 883–887.
[4] C. Rojas, J. Fine, L. Slipchenko, *J. Chem. Phys.* **2018**, *149*, 094103–094103.
[5] a) S. Gadre, A. Kulkarni, *Indian J. Chem.* **2000**, *39 A*, 50–59;b) S. Gadre, K. Babu, A. Rendell, *J. Phys. Chem. A* **2000**, *104*, 8976–8982;c) S. Gadre, K. Babu, *Resonance* **1999**, *4*, 11–20.
[6] H. Yu, W. van Gunsteren, *J. Chem. Phys.* **2004**, *121*, 9549–9564.
[7] a) R. Mulliken, *J. Chem. Phys.* **1955**, *23*, 1833–1840;b) A. Reed, R. Weinstock, F. Weinhold, *J. Chem. Phys.* **1985**, *83*, 735–746;c) P. Löwdin, *J. Chem. Phys.* **1950**, *18*, 365–375.
[8] F. Momany, *J. Phys. Chem.* **1978**, *82*, 592–601.
[9] a) L. Chirlian, M. Francl, *J. Comput. Chem.* **1987**, *8*, 894–905;b) U. Singh, P. Kollman, *J. Comput. Chem.* **1984**, *5*, 129–145;c) S. Cox, D. Williams, *J. Comput. Chem.* **1981**, *2*, 304–323;d) L. Chirlian, M. Francl, *J. Comput. Chem.* **1987**, *8*, 894–905.
[10] G. Hall, *Int. Rev. Phys. Chem.* **1986**, *5*, 115–120.
[11] M. Ramos, B. Webster, *J. Chem. Soc. Faraday Trans. 2*, **1983**, *79*, 1389–1398.
[12] A. Kumar, S. Gadre, N. Mohan, C. Suresh, *J. Phys. Chem. A* **2014**, *118*, 526–532.
[13] S. Gadre, R. Pathak, *Proc. Indian Acad. Sci. Chem. Sci.* **1990**, *102*, 189–192.
[14] S. Gadre, P. Bhadane, *Resonance* **1999**, *11*, 14–23.
[15] M. Leboeuf, A. Köster, K. Jug, D. Salahub, *J. Chem. Phys.* **1999**, *111*, 4893–4905.
[16] I. Shrivastava, S. Gadre, *Int. J. Quantum Chem.* **1994**, *49*, 397–407.
[17] a) S. Gadre, S. Pundlik, I. Shrivastava, *Proc. Indian Acad. Sci.* **1994**, *106*, 303–314;b) S. Gadre, I. Shrivastava, *Chem. Phys. Lett.* **1993**, *201*, 350–358.
[18] J. Albuquerque, R. Shirsat, *Int. J. Quantum Chem.* **2018**, DOI: 10.1002/qua.25853.
[19] Gaussian 03, Revision C.01, M. Frisch, G. Trucks, H. Schlegel, G. Scuseria, M. Robb, J. Cheeseman, J. Montgomery, Jr., T. Vreven, K. Kudin, J. Burant, J. Millam, S. Iyengar, J. Tomasi, V. Barone, B. Mennucci, M. Cossi, G. Scalmani, N. Rega, G. Petersson, H. Nakatsuji, M. Hada, M. Ehara, K. Toyota, R. Fukuda, J. Hasegawa, M. Ishida, T. Nakajima, Y. Honda, O. Kitao, H. Nakai, M. Klene, X. Li, J. Knox, H. Hratchian, J. Cross, C. Adamo, J. Jaramillo, R. Gomperts, R. Stratmann, O. Yazyev, A. Austin, R. Cammi, C. Pomelli, J. Ochterski, P. Ayala, K. Morokuma, G. Voth, P. Salvador, J. Dannenberg, V. Zakrzewski, S. Dapprich, A. Daniels, M. Strain, O. Farkas, D. Malick, A. Rabuck, K. Raghavachari, J. Foresman, J. Ortiz, Q. Cui, A. G. Baboul, S. Clifford, J. Cioslowski, B. Stefanov, G. Liu, A. Liashenko, P. Piskorz, I. Komaromi, R. Martin, D. Fox, T. Keith, M. Al-Laham, C. Peng, A. Nanayakkara, M. Challacombe, P. Gill, B. Johnson, W. Chen, M. Wong, C. Gonzalez, J. Pople, Gaussian, Inc., Wallingford CT, **2004**.
[20] R. Shirsat, S. Bapat, S. Gadre, *Chem. Lett. Phys.* **1992**, *200*, 373–378.
[21] T. Dyke, K. Mack, J. Muenter, *J. Chem. Physics* **1977**, *66*, 498–510.
[22] a) N. Silva, M. Adreance, M. Gordon, *J. Comput. Chem.* **2019**, *40*, 310–315; b) N. Kestner, M. Newton, T. Mathers, *Int. J. Quantum Chem.* **1983**, *17*, 431–439;c) M. Schütz, S. Brdarski, P. Widmark, R. Lindh, G. Karistrôm, *J. Chem. Phys.* **1997**, 107, 4597–4605;d) A. Mukhopadhyay, S. Xantheas, R. Saykally, *Chem. Phys. Lett.* **2018**, *700*, 163–175.
[23] a) A. Malloum, J. Fifen, Z. Dhaouadi, S. Engo, N. Jaidane, *Phys.Chem. Chem. Phys.* **2015**, *17*, 29226–29242;b) D. Hassett, C. Marsden, B. Smith, *Chem. Phys. Lett.* **1991**, *183*, 449–456;c) S. Gadre, S. Yeole, N. Sahu, *Chem. Rev.* **2014**, *114*, 12132–12173.
[24] E. Sälli, T. Salmi, L. Halonen , *J. Phys. Chem. A* **2011**, *115*, 11594–11605.
[25] A. Karpfen, *J. Phys. Chem. A* **1999**, *103*, 11431–11441.
[26] D. Tzeli, A. Mavridis, *J. Chem. Phys.* **2000**, *112*, 6178–6189.
[27] S. Burley, G. Petsko, *Science* **1985**, *229*, 23–28.
[28] C. Hunter, J. Sanders, *J. Am. Chem. Soc.* **1990**, *112*, 5525–5534.
[29] S. Tsuzuki, K. Honda, T. Uchimaru, M. Mikami, K. Tanable, *J. Am. Chem. Soc.* **2002**, *124*, 104–112.
[30] a) S. Tsuzuki, *Struc. Bond.* **2005**, *115*, 149–193;b) C. Enkvist, Y. Zhang, W. Yang, *Int. J. Quantum Chem.* **2000**, *79*, 325–329.
[31] a) T. Hofer, M. Wiedemair, *Phys. Chem. Chem. Phys.* **2018**, *20*, 28523–28534;b) X. Wang, S. Ramirez-Hinestrosa, J. Dobnikar, D. Frenkel, *Phys. Chem. Chem. Phys.* DOI: 10.1039/c9cp05445f.
[32] Subroutine STEPIT, written by J. Chandler, Physics Department, Indiana University, and distributed by QCPE, University of Indiana, Bloomington.